ORGANIC CHEMISTRY RESEARCH

Sulfonated Ethylenediamine Immobilized on Magnetic Nanoparticles as a Novel Heterogeneous Catalyst for the Green Preparation of 2-Arylbenzimidazoles

M. Fallah-Mehrjardi[a,b],* and H. Morovati[a]

[a]*Department of Chemistry, Payame Noor University (PNU), P. O. Box: 19395-3697, Tehran, Iran*
[b]*Research Center of Environmental Chemistry, Payame Noor University, Ardakan, Yazd, Iran*

Sulfonated ethylenediamine supported on silica-coated magnetite nanoparticles, $Fe_3O_4@SiO_2@(CH_2)_3$-en-SO_3H/H_2SO_4 as a new efficient solid acid catalyst was synthesized and fully characterized using various techniques such as FT-IR, FESEM, EDS, TEM, TGA, XRD and VSM. The resulting nanostructure catalyst was applied in the green synthesis of benzimidazole derivatives by the cyclocondensation reaction of o-phenylendiamine with aromatic aldehydes in refluxed ethanol and under solvent-free conditions. The nanocatalyst can be recovered magnetically and can be reused several times without a considerable loss in its catalytic activity.

INTRODUCTION

Functionalization of magnetic nanoparticles (MNPs) and immobilization of organic catalysts on the surface of MNPs are being widely studied in industries and academic centers because of their potential extensive applications in medicine, material science, chemistry and catalysis [1]. They can be classified as potent alternatives to the usual solid support materials for heterogenization of catalysts due to their diversity, availability, high surface area and easy functionalization. Magnetic nanocatalysts are easily separated from the reaction mixture using an external magnet without the need for other complex work-up procedures. These types of nanocatalysts are active, stable, reusable and environmentally friendly, which are very important in green chemistry [2-4].

Benzimidazole has two nitrogen atoms in the five-

membered ring, which is present in the structure of numerous natural products. The compounds possessing benzimidazole scaffold exhibit a wide range of biological and pharmaceutical activities such as anticancer, antimicrobial, anti-HIV, antifungal, antiviral and antibacterial activities [5-7]. In addition, derivatives of benzimidazole are also very important as inhibitors of angiotensin II [8], smooth muscle cell proliferation [9] and topoisomerase [10]. Also, they are very significant in organic syntheses [11-18]. There are various synthetic procedures for the synthesis of benzimidazole derivatives by the reaction of o-phenylenediamine with carboxylic acids or their derivatives and aldehydes [13]. Most of these methods have practical limitations such as the use of toxic materials and hazardous organic solvents, production of undesirable wastes and low atom economy. Therefore, there is still a need to develop green, efficient, simple and mild methods for the synthesis of 2-arylbenzimidazoles.

Given the catalytic importance of functionalized

---

*Corresponding author. E-mail: fallah.mehrjerdi@pnu.ac.ir

magnetic nanoparticles and in continuation of our previously reported articles for the synthesis of heterocyclic compounds [19-22], we now report the synthesis of a new nanomagnetic solid acid catalyst ($Fe_3O_4@SiO_2@(CH_2)_3$-en-SO_3H/H_2SO_4) and its characterization by various techniques. Moreover, the catalytic performance of the supported organocatalyst was studied in the cyclocondensation of arylaldehydes with *o*-phenylenediamine to 2-aryl benzimidazoles.

EXPERIMENTAL

General

All of the materials utilized in the present study were purchased from Sigma-Aldrich and Merck. Magnetite nanoparticles and silica-coated Fe_3O_4 NPs were prepared based on the previously reported methods [23]. Thin layer chromatography on silica gel polygram SILG/UV 254 plates were employed to monitor the reaction´s progress. All of the produced compounds were characterized by a comparison of their physical properties with authentic samples. Melting points were measured by an electrothermal 9200 apparatus in open capillary tubes. The different functional groups present in the synthesized compounds were confirmed by running their infrared spectra using KBr discs on a Shimadzu IRPrestige-21 spectrophotometer. The crystalline structure of nanoparticles was identified by XRD analysis using a PANalytical X'Pert Pro X-ray diffractometer. FESEM image and EDS spectrum of the catalyst nanoparticles were obtained with a Zeiss-Sigma VP microscope. TEM image of the catalyst was visualized with a Zeiss Em10C electron microscope. TGA was recorded on a TA-Q600 instrument under the air atmosphere in the temperature range of 25-800 °C at a rate of 10 °C min^{-1}. VSM was measured at room temperature on a Meghnatis Daghigh Kavir Co., Kashan, Iran.

Synthesis of Sulfonated Ethylenediamine Immobilized on Magnetite Nanoparticles

2 g of $Fe_3O_4@SiO_2$ was dispersed in toluene (100 ml) and ultrasonicated for 20 min. 2 ml of (3-chloropropyl) triethoxysilane was added into the mixture and stirred under reflux conditions for 12 h. The resulting $Fe_3O_4@SiO_2@(CH_2)_3$-Cl nanoparticles were separated magnetically, washed with EtOH and dried at 60 °C. Next, to a suspension of 2 g of $Fe_3O_4@SiO_2@(CH_2)_3$-Cl in acetonitrile (200 ml), 10 ml of ethylenediamine was added and stirred under reflux over 12 h. The resulting $Fe_3O_4@SiO_2@(CH_2)_3$-en nanoparticles were magnetically collected, washed with ethanol and dried at 60 °C. To a mixture of ethylenediamine immobilized on MNPs (2 g) in CH_2Cl_2 (50 ml), 2 ml of chlorosulfonic acid was added drop-wise and stirred at room temperature for 6 h to produce $Fe_3O_4@SiO_2@(CH_2)_3$-en-SO_3H/HCl that it was isolated magnetically, washed with EtOH and dried at 60 °C. To a mixture of produced MNPs (1.5 g) in water (20 ml), potassium hydrogen sulfate (excess, ~ 0.5 g) was added and stirred at room temperature overnight. The resultant product ($Fe_3O_4@SiO_2@(CH_2)_3$-en-SO_3H/H_2SO_4) was isolated magnetically, washed with EtOH and dried in vacuum.

Typical Procedure for the Synthesis of 2-Arylbenzimidazoles Catalyzed by $Fe_3O_4@SiO_2@(CH_2)_3$-en-SO_3H/H_2SO_4 in Ethanol

To a solution of *o*-phenylenediamine (1 mmol) and aromatic aldehydes (1 mmol) in EtOH (3 ml), the catalyst (0.01 g) was added and the mixture was stirred under reflux conditions for the appropriate time (Table 2). When the reaction was complete, as indicated by TLC (EtOAc:*n*-hexane 1:3), the nanocatalyst was removed in the presence of an external magnet. The mixture was then cooled down on ice, filtered off and recrystallized in aqueous ethanol (1:1, 5 ml) to give the desired products in high yields.

Typical Procedure for the Synthesis of 2-Arylbenzimidazoles Catalyzed by $Fe_3O_4@SiO_2@(CH_2)_3$-en-SO_3H/H_2SO_4 under Solvent-free Conditions

To a mixture of *o*-phenylenediamine (1 mmol) and aromatic aldehydes (1 mmol), the catalyst (0.01 g) was

added and stirred at 50 ºC for the appropriate time (Table 2). After the reaction was complete, as indicated by TLC (EtOAc:*n*-hexane 1:3), hot ethanol (5 ml) was added to the mixture and the nanocatalyst was removed in the presence of an external magnet. The mixture was then cooled down on ice, filtered off and recrystallized in aqueous ethanol (1:1, 5 ml) to give the desired products in high yields.

Selected Characterization Data

2-Phenyl-1*H*-benzimidazole (1). M.p. = 288-290 °C; IR (KBr): ῡ (cm^{-1}) 3048, 2962, 1443, 1408, 1277, 968, 741, 702; ^{1}H NMR (CDCl$_3$, 400 MHz): δ (ppm) 6.71-6.82 (m, 2H), 6.91-7.05 (m, 3H), 7.39-7.51 (m, 2H), 7.84-7.91 (m, 2H), 12.87 (br s, 1H); ^{13}C NMR (CDCl$_3$, 100 MHz): δ (ppm) 122.4, 126.1, 128.2, 128.9, 129.1, 129.7, 130.7, 152.1.

2-(4-Methylphenyl)-1*H*-benzimidazole (3). M.p. = 263-265 °C; IR (KBr): ῡ (cm^{-1}) 3049, 2961, 1441, 1407, 1275, 971, 750; ^{1}H NMR (CDCl$_3$, 400 MHz): δ (ppm) 2.26 (s, 3H), 7.21-7.26 (m, 2H), 7.34-7.39 (m, 2H), 7.43-7.57 (m, 2H), 7.81-7.89 (m, 2H), 12.64 (br s, 1H); ^{13}C NMR (CDCl$_3$, 100 MHz): δ (ppm) 23.4, 122.8, 123.2, 127.9, 128.7, 130.4, 143.4, 143.9, 153.4.

2-(2-Chlorophenyl)-1*H*-benzimidazole (4). M.p. = 229-231 °C; IR (KBr): ῡ (cm^{-1}) 3059, 2971, 1443, 1404, 1231, 972, 745; ^{1}H NMR (CDCl$_3$, 400 MHz): δ (ppm) 7.28-7.32 (m, 2H), 7.37-7.42 (m, 2H), 7.51-7.56 (m, 2H), 7.87-7.97 (m, 2H), 12.72 (br s, 1H); ^{13}C NMR (CDCl$_3$, 100 MHz): δ (ppm) 115.7, 123.4, 127.4, 128.1, 128.7, 129.4, 130.1, 137.9, 142.6, 152.9.

RESULTS AND DISCUSSION

The sulfonated ethylenediamine immobilized on magnetic nanoparticles (Fe$_3$O$_4$@SiO$_2$@(CH$_2$)$_3$-en-SO$_3$H/H$_2$SO$_4$) was prepared by a concise route depicted in Scheme 1. Silica-coated magnetite nanoparticles were prepared based on the reported procedure [23]. Then, (3-chloropropyl)triethoxysilane was added and refluxed in toluene. The nucleophilic attack of ethylenediamine to Fe$_3$O$_4$@SiO$_2$@(CH$_2$)$_3$-Cl led to the immobilization of
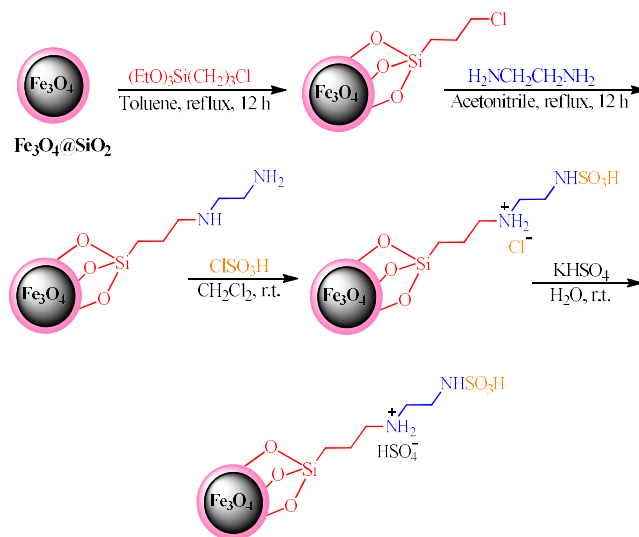
Scheme 1. The synthetic route for Fe$_3$O$_4$@SiO$_2$@(CH$_2$)$_3$-en-SO$_3$H/H$_2$SO$_4$ nanocatalyst

ethylenediamine on the surface of magnetic nanoparticles. The MNPs were sulfonated by the addition of chlorosulfonic acid and finally, the expected solid acid nanocatalyst (Fe$_3$O$_4$@SiO$_2$@(CH$_2$)$_3$-en-SO$_3$H/H$_2$SO$_4$) was produced by treatment with an aqueous solution of potassium hydrogen sulfate at room temperature.

The structure of the catalyst was explored by several techniques such as FT-IR, FESEM, EDS, TEM, VSM, TGA and XRD analyses. Important infrared spectral absorption vibrations of magnetic nanoparticles are presented in Fig. 1 in the form of a stacked spectrum. In the vibrational spectrum of the catalyst (Fe$_3$O$_4$@SiO$_2$@(CH$_2$)$_3$-en-SO$_3$H/H$_2$SO$_4$), a strong peak appeared at 559 cm^{-1} is assigned to the Fe-O stretching vibration and three important bands attributed to the Si-O-Si asymmetric stretching, symmetric stretching and bending vibrations are observed at 1080, 964 and 463 cm^{-1}, respectively. The entry of ethylenediamine is validated by the N-H bending absorption bands at 1512 cm^{-1}. The symmetric and asymmetric stretching absorption bands of O=S=O around 1050 to 1200 cm^{-1} overlapped with Si-O-Si asymmetric stretching vibrations. The presence of the broadband at 3414 cm^{-1}
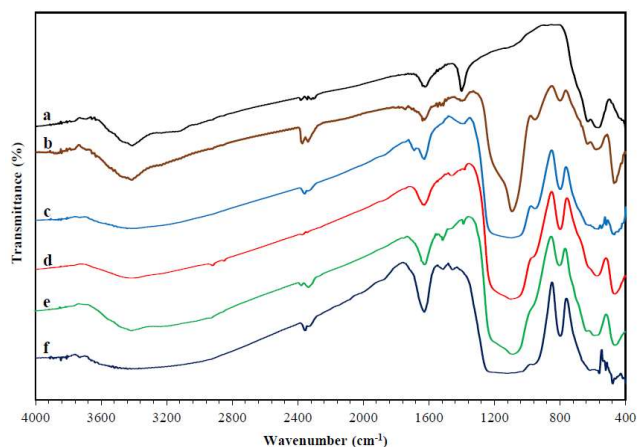
Fig. 1. A stacked infrared spectrum of (a) Fe_3O_4, (b) $Fe_3O_4@SiO_2$, (c) $Fe_3O_4@SiO_2@(CH_2)_3$-Cl, (d) $Fe_3O_4@SiO_2@(CH_2)_3$-en, (e) $Fe_3O_4@SiO_2@(CH_2)_3$-en-SO_3H/HCl and (f) $Fe_3O_4@SiO_2@(CH_2)_3$-en-SO_3H/H_2SO_4.

Fig. 2. FESEM image of $Fe_3O_4@SiO_2@(CH_2)_3$-en-SO_3H/H_2SO_4.

related to the O-H stretching absorption and O-H deformed vibration near 1628 cm^{-1} confirmed the existence of SO_3H moieties in the structure of the catalyst.

The FESEM image of $Fe_3O_4@SiO_2@(CH_2)_3$-en-SO_3H/H_2SO_4 shown in Fig. 2 indicates that the synthesized nanocatalyst has a nearly spherical morphology. Based on the SEM image, the particle size of the catalyst is less than 100 nm. Moreover, the TEM image confirmed the core-shell structure of the nanocatalyst and substantiated the results obtained from SEM (Fig. 3). The black dots in TEM image display the core of the Fe_3O_4 nanoparticles and introduce that the MNPs were successfully surrounded by a silica shell.

The EDS results obtained from the SEM analysis of the catalyst are presented in Fig. 4 and shows the presence of oxygen, iron, silicon, carbon, nitrogen and sulfur in the structure of the catalyst as expected. Au peak has been observed in EDX analysis because of the gold coating deposited on the samples before FESEM/EDX analysis.

Figure 5 shows the thermal stability of the synthesized catalyst determined by thermogravimetric analysis (TGA) which displays two-step weight loss steps over the temperature range of TG analysis (25-800 °C). The first
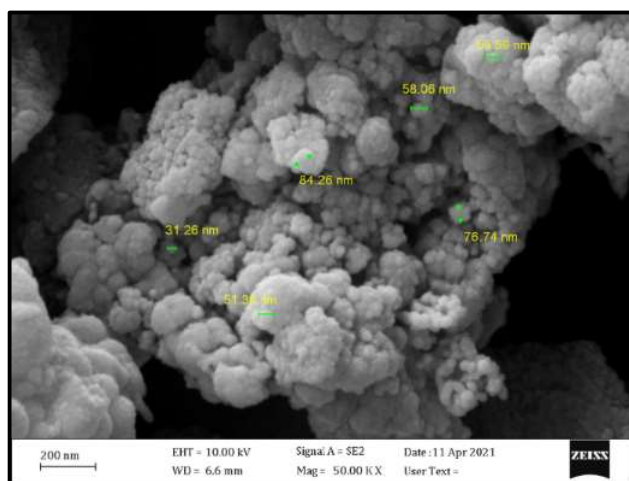

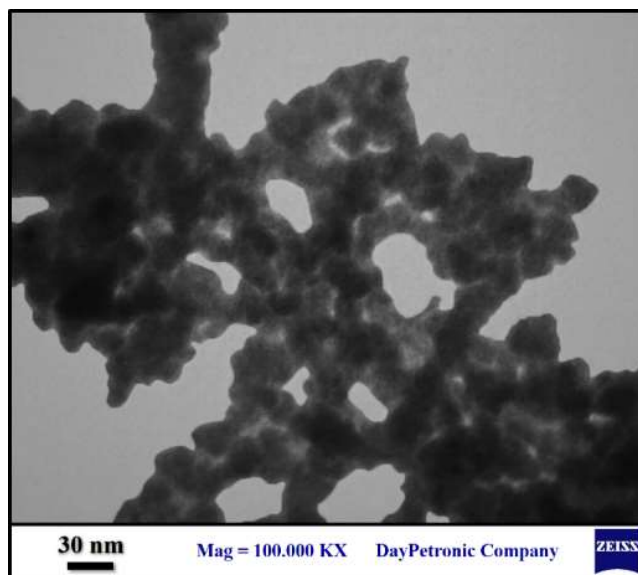**Fig. 3.** TEM image of $Fe_3O_4@SiO_2@(CH_2)_3$-en-SO_3H/H_2SO_4.

weight loss (~ 2.8 %) below 150 °C might be ascribed to the removal of physically absorbed water and hydroxyl groups on the surface of the catalyst. The second weight loss (~ 12.1 %) up to 200 °C can be ascribed to the breakdown and decomposition of organic moieties and thermal crystal phase transformation [24].
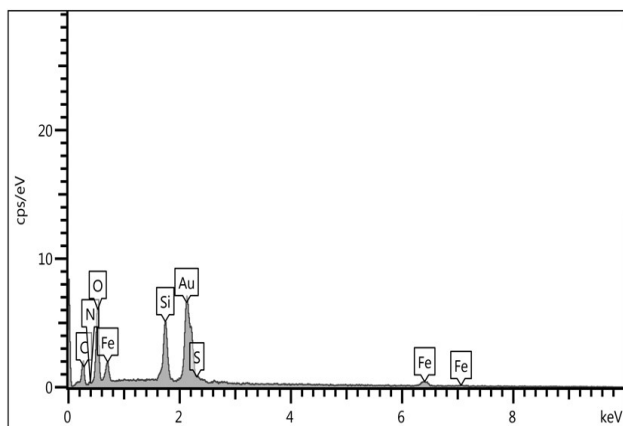
Fig. 4. EDS spectrum of $Fe_3O_4@SiO_2@(CH_2)_3$-en-SO_3H/H_2SO_4.
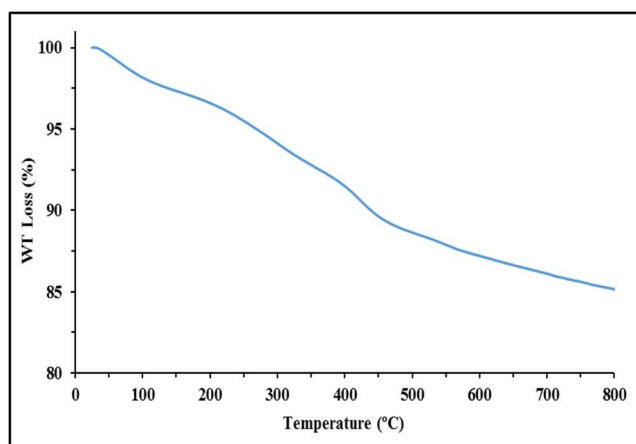
Fig. 5. TGA curve of $Fe_3O_4@SiO_2@(CH_2)_3$-en-SO_3H/H_2SO_4.

The crystalline degree of magnetite nanoparticles in the synthesized catalyst was obtained by XRD analysis in the 2θ region of 10-80° (Fig. 6). As can be seen in the XRD pattern, the intensity and positions of the diffraction peaks at 2θ = 30.40°, 35.72°, 43.30°, 53.97°, 57.35° and 63.04° are fully agree with the Fe_3O_4 pattern (2θ = 30.31°, 35.69°, 43.32°, 53.81°, 57.26° and 62.92°) [25].

The magnetic properties of the bare Fe_3O_4, $Fe_3O_4@SiO_2$ core-shell nanostructure and $Fe_3O_4@SiO_2@(CH_2)_3$-en-

SO_3H/H_2SO_4 nanocatalyst were investigated by a vibrating sample magnetometer (VSM) at ambient temperature (Fig. 7). The magnetic curves show that the saturation magnetization of the catalyst is 24 emu/g, which is much less than that of naked magnetic iron oxide (58 emu/g) and $Fe_3O_4@SiO_2$ (42 emu/g). The decrease in magnetic saturation of the catalyst is due to the presence of non-magnetic materials such as silica shell, linker and sulfonated ethylenediamine on the surface of nanoparticles.
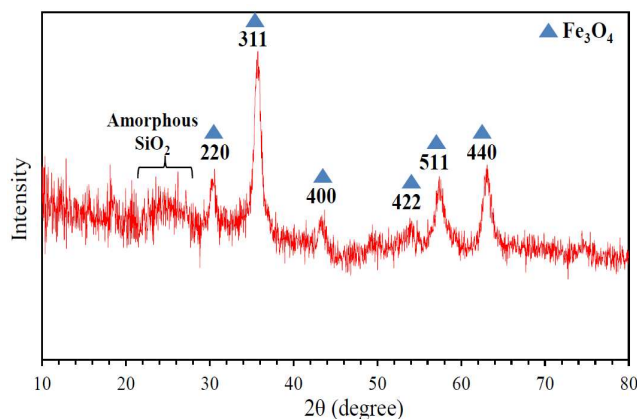

Fig. 6. XRD pattern of $Fe_3O_4@SiO_2@(CH_2)_3$-en-SO_3H/H_2SO_4.
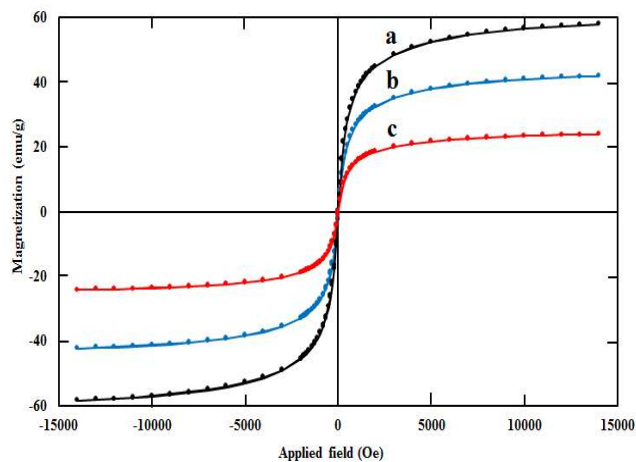
Fig. 7. The magnetization curves of (a) Fe_3O_4, (b) $Fe_3O_4@SiO_2$ and (c) $Fe_3O_4@SiO_2@(CH_2)_3$-en-SO_3H/H_2SO_4.

After successful synthesizing and characterizing the $Fe_3O_4@SiO_2@(CH_2)_3$-en-SO_3H/H_2SO_4, its catalytic efficiency was surveyed for the preparation of 2-arylsubstituted benzimidazoles. The reaction of benzaldehyde with *o*-phenylenediamine was chosen as a model reaction to obtain optimizing reaction conditions. After preliminary experiments, it was found that the best results are obtained when the reaction is carried out in refluxed ethanol or under solvent-free conditions in the presence of 0.01 g of the catalyst (Table 1).

As shown in Table 1, the reaction was incomplete in the absence of the catalyst. The rate of conversion was increased with the increase in the amount of catalyst and complete conversion was achieved when 0.01 g of the catalyst was used. The higher amount of the catalyst has no discernible influence on the rate of the reaction or the yield of the product. Also, by changing the reaction temperature in EtOH, it can be found that the rate of reaction is directly proportional to temperature and the best results were observed under reflux conditions (Table 1, Entry 6). Due to the importance of organic syntheses in neat conditions, this reaction was also investigated under solvent-free conditions, which showed that the reaction at 50 °C was completed after 1 h (Table 1, Entry 12).

After obtaining the optimal conditions, we then evaluated the generality of these conditions to other aromatic aldehydes with electron-donating and electron-withdrawing substituents (Scheme 2, Table 2). It is obvious from Table 2 that all of the studied arylaldehydes were completely converted into their respective 2-arylbenzimidazoles in short reaction times and with high isolated yields. Interestingly, only 2-arylbenzimidazoles are produced in all cases under the optimal conditions and when two equivalents of benzaldehyde are employed, the di-substituted benzimidazoles are obtained as a by-product.

To check the constancy of the catalyst activity, the catalyst was reused five times in the condensation reaction between benzaldehyde and *o*-phenylenediamine in refluxed ethanol. The catalyst was magnetically separated from   the

Table 1. Optimization of the Reaction Conditions in the Model Reaction[a]

Entry	Catalyst (g)	Solvent/conditions	Time (min)	Yield (%)
1	0.01	H_2O/reflux	60	Trace
2	0.01	EtOAc/reflux	60	Trace
3	0.01	CH_2Cl_2/reflux	60	Trace
4	0.01	$CHCl_3$/reflux	60	40
5	0.01	MeCN/reflux	60	65
6	0.01	EtOH/reflux	20	92
7	-	EtOH/reflux	60	Trace
8	0.02	EtOH/reflux	18	93
9	0.01	EtOH/r.t.	60	40
10	0.01	EtOH/60 °C	60	70
11	0.01	Solvent-free, r.t.	60	43
12	0.01	Solvent-free, 50 °C	25	93
13	0.01	Solvent-free, 75 °C	22	92
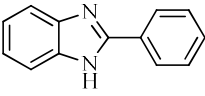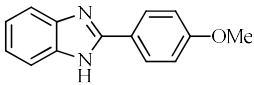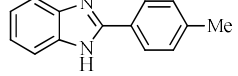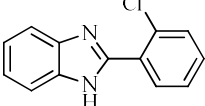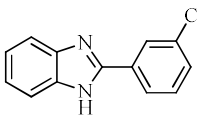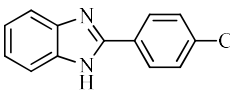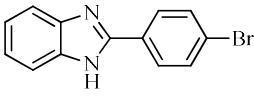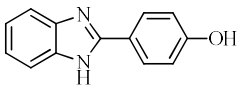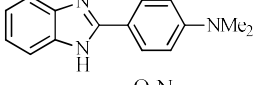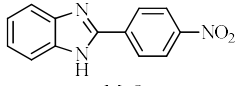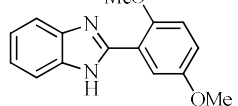
[a]Reaction conditions: benzaldehyde (1 mmol), *o*-phenylenediamine (1 mmol), catalyst, solvent (3 ml).
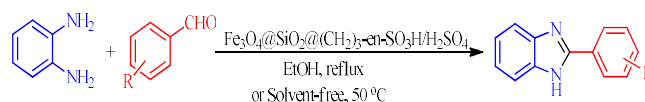
Scheme 2. Synthesis of 2-arylbenzimidazoles in the presence of $Fe_3O_4@SiO_2@(CH_2)_3$-en-SO_3H/H_2SO_4
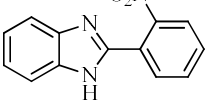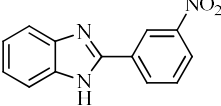
reaction mixture after each run, washed with ethanol and acetone, dried in an oven at 60 °C for an hour and reused in the subsequent run. Very low reduction in the product yields (92%, 92%, 89%, 86%, and 85% in cycles 1-5, respectively) indicated that the catalyst can be recycled and reused at least five times without a significant decrease in its activity (Fig. 8).

Table 2. Synthesis of 2-Arylbenzimidazoles Catalyzed by $Fe_3O_4@SiO_2@(CH_2)_3$-en-SO_3H/H_2SO_4

Entry	Product	In ethanol Time (min)/Yield (%)[a]	Solvent-free Time (min)/Yield (%)[a]	m.p. (°C) Found	m.p. (°C) Reported [Ref.]
1		20/92	25/93	288-290	292-294 [17]
2		25/91	30/90	222-224	222-224 [18]
3		22/90	30/88	263-265	260-262 [17]
4		30/89	35/90	229-231	230-232 [18]
5		25/87	30/89	194-195	194-196 [16]
6		20/90	20/92	285-287	289-291 [14]
7		20/88	25/89	279-281	268-270 [17]
8		22/85	30/85	236-238	234-236 [18]
9		25/87	30/88	271-272	276-278 [14]
10		20/89	25/91	262-264	260 [26]
11		18/90	20/86	186-188	186-188 [26]
12		15/87	25/91	> 300	315-317 [26]
13		25/86	30/85	211-214	212-214 [16]

[a]Isolated yields.
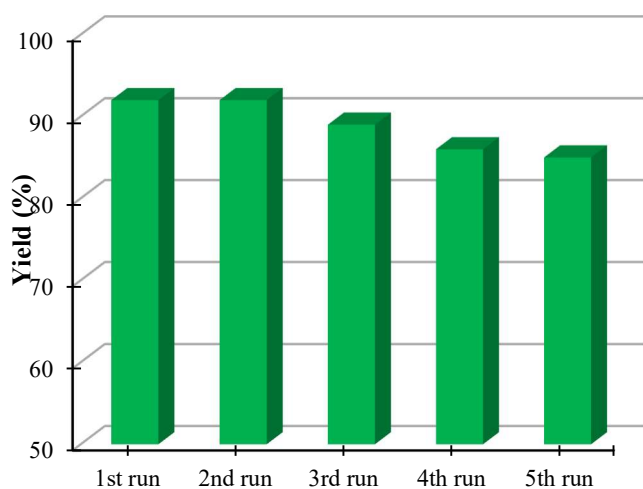
Fig. 8. Recyclability of the catalyst.

The comparison of the efficacy of $Fe_3O_4@SiO_2@(CH_2)_3$-en-SO_3H/H_2SO_4 in the condensation between *o*-phenylenediamine and benzaldehyde along with a few protocols already documented in the previous manuscripts is presented in Table 3. It is revealed from the results obtained that the present technique overcomes the drawbacks of the previously reported methodologies and has dominance because of the high percentage yield, shorter reaction time and the amount of catalyst loaded.

CONCLUSION

In conclusion, sulfonated ethylenediamine was successfully supported on the surface of silica-coated nanomagnetite and was fully characterized by various techniques. The magnetic nanocomposite was then utilized in the synthesis of 2-arylbenzimidazoles by the condensation reaction of various aromatic aldehydes with *o*-phenylenediamine. The present method has many advantages over the previously reported procedures in terms of reduced reaction timings, higher yield, simplicity in operation and work-up, avoiding the application of dangerous acids or bases, simple recovery of the nanomagnetic catalyst and reuse of the catalyst several times without a remarkable decrease in its activity.

ACKNOWLEDGEMENTS

REFERENCES

[1] V. Polshettiwar, R. Luque, A. Fihri, H. Zhu, M. Bouhrara, J.-M. Basset, Chem. Rev. 111 (2011) 3036.

Table 3. A Comparative Analysis of Effectiveness of Different Catalysts for the Preparation of 2-Pheylbenzimidazole

Entry	Catalyst	Conditions	Time (min)	Yield (%)	Ref.
1	*p*-TsOH	DMF/80 °C	10	85	[12]
2	$VOSO_4$	EtOH/r.t.	60	92	[14]
3	Silica sulfuric acid	EtOH/reflux	20	91	[15]
4	$Fe_3O_4@SiO_2$-SO_3H	EtOH, reflux	20	91	[16]
5	Nano-γ-alumina	EtOH/reflux	90	88	[17]
6	$TiCl_3OTf$	EtOH/r.t.	70	84	[18]
7	Au/TiO_2	$CHCl_3$:MeOH/r.t.	120	98	[27]
8	$Fe_3O_4@SiO_2@(CH_2)_3$-en-SO_3H/H_2SO_4	EtOH/reflux	20	92	-[a]
9	$Fe_3O_4@SiO_2@(CH_2)_3$-en-SO_3H/H_2SO_4	Neat/50 °C	25	93	-[a]

[a]This work.

[2]   W. Ma, A.G. Ebadi, M.S. Sabil, R. Javahershenas, G. Jimenez, RSC Adv. 9 (2019) 12801.

[3]   G. Feng, D. Hu, L. Yang, Y. Cui, X.A. Cui, H. Li, Sep. Purif. Technol. 74 (2010) 253.

[4]   J. Davarpanah, A.R. Kiasat, Catal. Commun. 42 (2013) 98.

[5]   D. Carcanague, Y.K. Shue, M.A. Wuonola, M. Uria-Nickelsen, C. Joubran, J.K. Abedi, J. Jones, T.C. Kühler, J. Med. Chem. 45 (2002) 4300.

[6]   Y. Özkay, Y. TunalI, H. Karaca, I. IşIkdağ, Arch. Pharm. Res. 34 (2011) 1427.

[7]   N. Shrivastava, M.J. Naim, M.J. Alam, F. Nawaz, S. Ahmed, O. Alam, Arch. Pharm. 350 (2017) 1.

[8]   Y. Kohara, K. Kubo, E. Imamiya, T. Wada, Y. Inada, T. Naka, J. Med. Chem. 39 (1996) 5228.

[9]   S.Y. Hong, K.H. Chung, H.J. You, I.H. Choi, M.J. Chae, J.Y. Han, O.J. Jung, S.J. Kang, C.K. Ryu, Bioorganic Med. Chem. Lett. 14 (2004) 3563.

[10] Q. Sun, B. Gatto, C. Yu, A. Liu, L.F. Liu, E.J. LaVoie, J. Med. Chem. 38 (1995) 3638.

[11] B.Y. Yinjuan Bai, J. Lu, Z. Shi, Synlett (2001) 544.

[12] H. Xiangming, M. Huiqiang, W. Yulu, Arkivoc (2007) 150.

[13] S.I. Alaqeel, J. Saudi Chem. Soc. 21 (2017) 229.

[14] C.S. Digwal, U. Yadav, A.P. Sakla, P.V. Sri Ramya, S. Aaghaz, A. Kamal, Tetrahedron Lett. 57 (2016) 4012.

[15] B. Sadeghi, M. Ghasemi Nejad, J. Chem. (2013) 581465.

[16] M. Fallah-Mehrjardi, M. Ayazi, S.H. Banitaba, Iran. Chem. Commun. 8 (2020) 80.

[17] A. Teimouri, A.N. Chermahini, H. Salavati, L. Ghorbanian, J. Mol. Catal. A Chem. 373 (2013) 38.

[18] J. Azizian, P. Torabi, J. Noei, Tetrahedron Lett. 57 (2016) 185.

[19] M. Beyki, M. Fallah-Mehrjardi, Lett. Org. Chem. 15 (2017) 39.

[20] F. Najafi, M. Fallah-Mehrjardi, Lett. Org. Chem. 15 (2018) 778.

[21] H. Talaei, M. Fallah-Mehrjardi, F. Hakimi, J. Chinese Chem. Soc. 65 (2018) 523.

[22] M. Fallah-Mehrjardi, S. Kalantari, Org. Chem. Res. 6 (2020) 137.

[23] A.R. Kiasat, J. Davarpanah, J. Mol. Catal. A. Chem. 373 (2013) 46.

[24] M.Z. Kassaee, H. Masrouri, F. Movahedi, Appl. Catal. A Gen. 395 (2011) 28.

[25] M. Fallah-Mehrjardi, S. Kalantari, Russ. J. Org. Chem. 56 (2020) 298.

[26] H. Ghafuri, E. Esmaili, M. Talebi, C.R. Chimie 19 (2016) 942.

[27] M.A. Tzani, C. Gabriel, I.N. Lykakis, Nanomaterials 10 (2020) 2405.